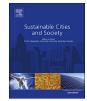
Contents lists available at ScienceDirect





Sustainable Cities and Society

journal homepage: www.elsevier.com/locate/scs

# The study of thermal pattern changes using Landsat-derived land surface temperature in the central part of Isfahan province



Maliheh Madanian<sup>a</sup>, Ali Reza Soffianian<sup>a,\*</sup>, Saeid Soltani Koupai<sup>a</sup>, Saeid Pourmanafi<sup>a</sup>, Mehdi Momeni<sup>b</sup>

months

<sup>a</sup> Department of Natural Resources, Isfahan University of Technology, 8415683111, Isfahan, Iran
<sup>b</sup> Remote Sensing Division, Geomatic Engineering, University of Isfahan, 81746-73441, Isfahan, Iran

ARTICLEINFO	A B S T R A C T
Keywords: Land-use/land-cover Land surface temperature (LST) Surface urban heat island (SUHI) Surface urban cool island (SUCI) Isfahan	Urban development and consequently, the growth of construction can result in changing the climatic para- meters, such as land surface temperature (LST). This study was conducted in the central part of Isfahan province to investigate changes in thermal patterns during 1985–2015 time period. To generate land-use/land-cover maps and LST, Landsat-TM, ETM+ and OLI/TIRS data were utilized. The results demonstrated that impervious sur- faces had been increased by 2.8 times from 1985 to 2015. The results also indicated a negative correlation between LST and the Normalized Difference Vegetation Index (NDVI) in hot months. This research also focused on exploring the occurrence of surface urban heat island (SUHI) in hot and cold months in the city of Isfahan. Buffer zones in various widths were created to measure SUHI. In August 1985, in buffers of 1 km–3 km and in July 1992, in all buffers, SUHI was observed. In contrast, in July 2001, in buffers of 3 km–10 km and in July 2015, in all buffers, LST of Isfahan rural area was higher than that of city, showing surface urban cool island (SUCI). The results also demonstrated that the urban area was cooler than the surrounding rural area in the cold

## 1. Introduction

Development of urban areas causes extensive changes in the land surfaces, leading to the local climate change (Changnon, 1978, 1992; Landsberg, 1970). Urbanization and anthropogenic activities lead to the vast replacement of soil and vegetation with pavements, building structures, and dark surfaces with urban materials (concrete, asphalt and metal) (Ngie, Abutaleb, Ahmed, Darwish, & Ahmed, 2014). The replacement of natural zones or vegetation by impervious surfaces has changed the exchange of energy between soil and atmosphere. So microclimatic variables such as temperature and winds near the surface have been changed (Jin, Dickinson, & Zhang, 2005). The local atmosphere and also, land surface temperature (LST) due to the quick growth of urban areas have experienced changes, as compared to the surrounding areas (Chakraborty, Kant, & Mitra, 2015). These changes modify the climatic balance, producing a new climate called the urban climate (Landsberg, 1981; Oke, 1987; Oke, Zeuner, & Jauregui, 1992; Wanner & Hertig, 1984). The surface temperature is an important factor in the study of urban climate (Voogt & Oke, 2003).

When the temperature of large cities is compared with that of the

surrounding areas, two phenomena are observed: the higher temperature, referred to as urban heat island (UHI), and the occasionally lower temperature known as urban cool island (UCI) (Memon, Leung, & Liu, 2008). The urban heat island (UHI) is known as a phenomenon in which surface and atmospheric modifications, owing to urbanization, can result in the modified thermal climate, by being warmer in the urban area than the surrounding non-urbanized ones (Voogt & Oke, 2003). No absorption of water by construction materials and therefore, absence of evapotranspiration, and also, further absorption and retention of sun's heat by the impervious surfaces, as compared to natural vegetation, are among the major reasons for the higher temperature in the residential areas (Gartland, 2008). Among the harmful effects of UHI, the increase of energy consumption (Konopacki & Akbari, 2002), the rise of groundlevel ozone (Rosenfeld, Akbari, Romm, & Pomerantz, 1998), the reduction of quality of life environment, and the growing mortality rate (Changnon, Kunkel, & Reinke, 1996) can be mentioned. In contrast, surface urban cool island (SUCI) is defined as an urban area with a lower temperature than the non-urban surrounding areas, which is usually the case in arid and semi-arid regions (Guoyin & Mingyi, 2009; Shigeta, Ohashi, & Tsukamoto, 2009). The results of previous studies

\* Corresponding author.

https://doi.org/10.1016/j.scs.2018.03.018 Received 10 May 2017; Received in revised form 25 November 2017; Accepted 17 March 2018 Available online 28 March 2018 2210-6707/ © 2018 Elsevier Ltd. All rights reserved.

*E-mail addresses:* m.madanian@na.iut.ac.ir (M. Madanian), soffianian@cc.iut.ac.ir (A.R. Soffianian), ssoltani@cc.iut.ac.ir (S. Soltani Koupai), Spourmanafi@cc.iut.ac.ir (S. Pourmanafi), momeni@eng.ui.ac.ir (M. Momeni).

showed UCI was due to irrigated gardens in the city cores (Schwarz, Schlink, Franck, & Großmann, 2012), the high amount of vegetation in urban areas, as compared to suburban areas where the bare ground and sand are more abundant (Lazzarini, Marpu, & Ghedira, 2013), and barren soils with a higher temperature in the surrounding rural areas than the urban ones(Haashemi, Weng, Darvishi, & Alavipanah, 2016).

Satellite-measured LST is typically utilized to identify SUHI (Yuan & Bauer, 2007). Satellite imagery, due to features such as spatial coverage and temporal repetition, are useful for showing the spatial patterns of the urban thermal environment (Li, Zhang, & Kainz, 2012). Considerable studies have been conducted on UHI using different satellite images. Weng and Lu (2008) utilized Landsat TM/ETM+ images. showing that there was a thermal gradient from the Central Business District of Indianapolis, USA (CBD), outward into the countryside. Mallick, Rahman, and Singh (2013), by employing satellite images of ASTER and Landsat ETM+, estimated UHI intensity to be greater than 4 °C between the Central Business District of Delhi and commercial/ industrial areas, as compared to the suburbs. Feng, Zhao, Chen, and Wud (2014) applied Landsat TM/ETM+ data, finding a trend of continuous increase in UHI from 0.83 °C to 2.14 °C during the period studied in Xiamen City, China. Shen, Huang, Zhang, Wuc, and Zeng (2016) used Landsat, MODIS and AVHRR data to obtain the maximum temperature difference between the city zone and the rural area; it was 7.19 K for the old city zone, and 4.65 K for the area within the third ring road in the city of Wuhan, China. In contrast, fewer studies have been carried out on SUCI that has occurred in arid and semi-arid regions. Haashemi et al. (2016) studied seasonal SUHI fluctuations in Tehran as a semi-arid city. The results indicated the occurrence of SUCI during the daytime with the maximum difference of -4 Kelvin (K) in March and SUHI at night. In another study conducted by Lazzarini et al. (2013), in the desert city of Abu Dhabi, the downtown area was colder than the suburbs in summer, between 5–6 K; in winter, this difference was 2–3 K. Rasul, Balzter, & Smith, (2016) also investigated the temporal formation of daily SUCI and night-time SUHI in Erbil, Iraq, which is a region with a semi-arid climate. The results demonstrated that the residential areas during the day in summer, autumn and winter had a lower LST in comparison to the surrounding areas. In contrast, at night-time, a higher LST was observed, and SUHI was detected. In a study carried out by Xian and Crane (2006), the daily cooling effect in Las Vegas was observed.

The objectives of this study were: 1) to identify LST distribution patterns in hot and cold months within the central part of Isfahan province using Landsat-5 TM, Landsat-7 ETM + and Landsat-8 OLI/TIRS data during the 1985–2015 period; 2) to investigate the relationship between LST and land-use/land-cover types and NDVI (Normalized Difference Vegetation Index); and 3) to explore the occurrence of SUHI in Isfahan city and the resulting changes during the time studied.

#### 2. Study area

The study area (Fig. 1) is located in the central part of Isfahan province, Iran, covering several cities such as Isfahan, Khomeinishahr, Najafabad, Falavarjan, Mobarakeh and Shahinshahr (black circles in Fig. 1). Isfahan province is located between 30°42′–34°27′N and 49°38′–55°32′E, covering 107045 km<sup>2</sup>. This province covers 24 townships (Isfahan Governorship website). In recent decades, some kind of urban expansion has occurred in different cities of the province. The population of Isfahan province was increased from 3288734 in 1986 and to 4879312 in 2011 (Statistical center of Iran, 2011). Weather in Isfahan province is generally a moderate dry one, but due to the effect of winds and the proximity to mountainous areas in the west, Kavir plain in the east and southeast, it can be classified in to three distinct zones: 1) arid weather, 2) semi-arid weather, and 3) semi-humid cold weather. Weather in Isfahan Township is a semi-desert one characterized by dryness and little rainfall (Iran's meteorological organization

website). The average temperature in this province, from west to east, has been increased. This average is around 4 °C in the high altitudes and in the eastern parts, it is around 22 °C. The average annual rainfall of the province is ranging from 1300 mm in the western altitudes to 60 mm in the east and northeastern parts. Overall, the average rainfall in Isfahan province has been around 150 mm (in a period of 36 years) (Khodaghli, 2008).

#### 3. Data and methods

In this study, Landsat thematic mapper (TM), Enhanced Thematic Mapper Plus (ETM+), and Operational Land Imager and Thermal Infrared Sensor (OLI/TIRS) imagery acquired in 1985, 1992, 2001, and 2015 with the cloud coverage of less than 10% were used (Table 1). Clouds which were mainly in rocks and bare lands were masked out. All images had been already rectified by USGS to the Universal Transverse Mercator (UTM) projection system, WGS84, zone 39N, such that a rootmean-square error (RMSE) less than half of a pixel was acceptable (Lunetta, Lyon, Guindon, & Elvidge, 1998). Radiometric and atmospheric corrections were performed prior to land-use/land-cover classification. For the retrieval of land surface temperature, the top-of-atmosphere (TOA) reflectance was used.

Land-use/land-cover classification was performed using the Support Vector Machine (SVM) technique and NDVI index. Finally, maps were created in six land-use/land-cover types, i.e., impervious surface, vegetation, harvested agricultural land, others, water, and road (Table 2), with the overall accuracy range being between 85%–91%. For conducting the subsequent analyses, two classes of impervious surface and road were merged into one. Since there were no considerable changes in the impervious surfaces in the interval between hot and cold months of each year, this category was assumed to be the same in the two Landuse/land-cover maps created for each year.

## 3.1. Retrieval of land surface temperature

In this study, thermal bands of Landsat TM, ETM + and OLI/TIRS (band 6, band 6/1 and band 10, respectively) were utilized to map LST. In the first step, at-sensor spectral radiance was estimated, such that digital numbers (DN) were converted to the physically meaningful common radiometric scale using Eq. (1) for Landsat-5,7 (Chander, Markham, & Helder, 2009) and Eq. (2) for Landsat-8 (USGS website), respectively:

$$L_{\lambda} = \left(\frac{LMAX_{\lambda} - LMIN_{\lambda}}{Q_{calmax} - Q_{calmin}}\right) (Q_{cal} - Q_{calmin}) + LMIN_{\lambda}$$
(1)

where  $L_{\lambda}$  refers to the spectral radiance at the sensor's aperture in W/ (m<sup>2</sup> sr  $\mu m$ ),  $Q_{cal}$  is the quantized calibrated pixel value (DN),  $Q_{calmin}$  is the minimum quantized calibrated pixel value corresponding to LMIN\_{\lambda},  $Q_{calmax}$  is the maximum quantized calibrated pixel value corresponding to LMAX\_{\lambda}, LMIN\_{\lambda} is the spectral at-sensor radiance scaled to  $Q_{calmax}$  in W/(m<sup>2</sup> sr  $\mu m$ ), and LMAX\_{\lambda} is the spectral at-sensor radiance scaled to  $Q_{calmax}$  in W/(m<sup>2</sup> sr  $\mu m$ ).

$$L_{\lambda} = M_L Q_{cal} + A_L \tag{2}$$

where  $M_L$  refers to band-specific multiplicative rescaling factor,  $A_L$  is band-specific additive rescaling factor provided in the product metadata file, and  $Q_{cal}$  refers to quantized and calibrated standard product pixel values (DN).

In the second step, by assuming that earth's surface is a black body with the spectral emissivity of 1, at-sensor spectral radiance was converted to effective at-sensor brightness temperature according to Eq. (3) (Chander et al., 2009):

$$T_B = \frac{K_2}{\ln\left(\frac{K_1}{L_\lambda} + 1\right)} \tag{3}$$

Download English Version:

# https://daneshyari.com/en/article/6775483

Download Persian Version:

https://daneshyari.com/article/6775483

Daneshyari.com